Available online at www.sciencedirect.com
SCIENCE DIRECT®
Biochemical and Biophysical Research Communications 338 (2005) 215–222
BBRC
www.elsevier.com/locate/ybbrc

Molecular basis for the substrate selectivity of bicyclic and monocyclic extradiol dioxygenases ☆

Frédéric H. Vaillancourt [a,b,c,1], Pascal D. Fortin [a,b,c], Geneviève Labbé [a,b,c,2], Nathalie M. Drouin [c,3], Zamil Karim [a,b], Nathalie Y.R. Agar [c,4], Lindsay D. Eltis [a,b,c,*]

[a] Department of Microbiology, University of British Columbia, Vancouver, BC, Canada V6T 1Z3
[b] Department of Biochemistry, University of British Columbia, Vancouver, BC, Canada V6T 1Z3
[c] Department of Biochemistry, Pavillon Marchand, Université Laval, Quebec City, Que., Canada G1K 7P4

Received 27 June 2005
Available online 8 September 2005

Abstract

Extradiol dioxygenases play a key role in determining the specificities of the microbial aromatic catabolic pathways in which they occur. To identify the structural determinants of specificity in this class of enzymes, variants of 2,3-dihydroxybiphenyl (DHB) 1,2-dioxygenase (DHBD) were investigated. Structural data of the DHBD/DHB complex informed the design of seven variants at four positions: V148W, V148L, M175W, A200I, A200W, P280W, and V148L/A200I. All variants had reduced specificity for DHB. In addition, the V148W, V148L, A200I, and V148L/A200I variants had increased specificity for catechol. Indeed, the V148W variant had a higher apparent specificity for 3-Me catechol than for DHB, although the substitution reduced the k_{cat} for all tested substrates as well as the rate constant of suicide inactivation of the enzyme. These results are consistent with available structural data which suggest that the larger residue at position 148 may partially occlude O_2 binding. The results further indicate that in addition to defining substrate specificity, the binding pocket orientates the bound catechol to minimize oxidative inactivation of the enzyme during catalysis.

Keywords: Extradiol; Dioxygenase; Enzymology; Inactivation

Bacteria have evolved a variety of strategies to degrade aromatic compounds, all of which involve the activation of the aromatic ring followed by its cleavage [1–3]. One widespread aerobic degradation strategy involves the generation of a catecholic intermediate possessing hydroxyl substituents on adjacent carbon atoms which is then subject to oxygenolytic ring-cleavage [3]. The ring-cleavage reaction is performed by enzymes from one of two structurally and mechanistically distinct classes [4]. Both types of enzymes were originally purified and characterized by Hayaishi and co-workers [5,6]. Intradiol dioxygenases utilize non-heme Fe(III) to cleave the aromatic nucleus *ortho* to (between) the hydroxyl substituents. In contrast, extradiol dioxygenases utilize non-heme Fe(II) to cleave the aromatic nucleus *meta* (adjacent) to the hydroxyl substituents (Fig. 1). Mn(II)-dependent extradiol dioxygenases with strong sequence similarity to the Fe(II) counterpart have also been reported [7].

Sequence and structural data indicate the existence of at least two evolutionarily independent types of extradiol dioxygenases [8,9]. The type I extradiol dioxygenases

☆ *Abbreviations:* C23O, catechol 2,3-dioxygenase; DHB, 2,3-dihydroxybiphenyl; DHBD, 2,3-dihydroxybiphenyl 1,2-dioxygenase; HEPPS, 4-(2-hydroxyethyl)-1-piperazinepropanesulfonic acid; HPLC, high performance liquid chromatography; SDS, sodium dodecyl sulfate.

* Corresponding author. Fax: +1 604 822 6041.
E-mail address: leltis@interchange.ubc.ca (L.D. Eltis).
[1] Present address: Department of Biological Chemistry and Molecular Pharmacology, Harvard Medical School, Boston, MA 02115, USA.
[2] Present address: Department of Chemistry, University of Waterloo, Waterloo, Ont., Canada N2L 3G1.
[3] Present address: ID Biomedical Corporation of Quebec, Laval, Que., Canada H7V 3S8.
[4] Present address: Department of Neurosurgery, Brigham and Women's Hospital, Harvard Medical School, Boston, MA 02115, USA.

0006-291X/$ - see front matter © 2005 Published by Elsevier Inc.
doi:10.1016/j.bbrc.2005.08.219

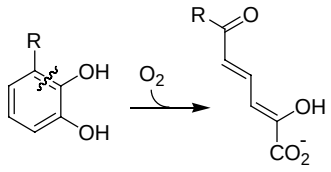

Fig. 1. Reaction catalyzed by extradiol dioxygenases. In the aerobic catabolism of biphenyl, DHBD catalyzes a reaction in which R = phenyl. In the aerobic catabolism of several aromatics proceeding via catechol, C23O catalyzes a reaction in which R = H. The latter reaction, including its product, was first described by Hayaishi and co-workers [6].

belong to the vicinal oxygen chelate superfamily [10,11] and can be one- or two-domain enzymes. Each domain contains two copies of a βαβββ module [12], and phylogenetic analyses indicate that the enzymes share a common one-domain ancestor [8]. Divergence among the two-domain dioxygenases has resulted in several families, at least two of which are based on substrate preference. For example, 2,3-dihydroxybiphenyl 1,2-dioxygenase (DHBD) from *Burkholderia xenovorans* LB400 [13–15] belongs to a family with a preference for bicyclic substrates. In contrast, catechol 2,3-dioxygenase (C23O) from *Pseudomonas putida* mt-2 [16], the enzyme originally described by Hayaishi and co-workers [6], belongs to a family with a preference for monocyclic substrates.

Several studies have demonstrated that type I extradiol dioxygenases play a key role in determining the specificities of the catabolic pathways in which they occur. For example, the specificity of C23O prevents the growth of *P. putida* mt-2 on 4-ethylbenzoate and corresponding xylenes [17]. The specificity of DHBD similarly prevents the bacterial degradation of certain PCB congeners [18,19]. Sub-optimal substrates are cleaved with low specificity (k_{cat}/K_m) and can also accelerate the oxidative inactivation of the enzyme during catalytic turnover. This suicide inactivation appears to be due to the dissociation of superoxide from the enzyme:catechol:dioxygen ternary complex to ultimately yield an inactive Fe(III) enzyme [20]. Inactivation thus competes with ring-cleavage and is reflected in the partition coefficient, the ratio of k_{cat} to j_3, the rate constant of inactivation. Electronic factors clearly play a significant role in determining the magnitudes of k_{cat} and j_3. For example, C23O is rapidly inactivated by 3-chlorocatechol yet efficiently cleaves the isosteric 3-methylcatechol [21]. However, it is also clear that steric factors influence the partition coefficient as catechol inactivates DHBD much quicker than DHB [20].

Herein, a series of seven variants of DHBD were generated using site-directed mutagenesis to investigate the molecular basis for the substrate selectivity between DHBD and C23O. All DHBD variants were purified and steady-state kinetics with 2,3-dihydroxybiphenyl (DHB) and catechol were performed. The two variants showing the biggest improvement toward catechol were further characterized with respect to their specificities for other catechols and their inactivation parameters. The results are discussed using the available structures of type I extradiol dioxygenases.

Materials and methods

Chemicals. DHB [22] and 3-Cl catechol were gifts from Victor Snieckus (Dept. of Chemistry, Queen's University, Ont., Canada). Ferene S was from ICN Biomedicals Inc. All other chemicals were of analytical grade and used without further purification.

Construction of plasmids and overexpression of protein. DNA was manipulated using standard protocols [23]. All oligonucleotides used in this study are described in Table 1. Site-directed mutagenesis was performed via restriction site elimination [24] using a vector containing the 3′ half *bphC* gene and oligo oODM (Table 1) to remove an *Eco*RI restriction site from the multiple cloning site. Briefly, the *bphC* gene was amplified by PCR using oligos obphC-for-*Nco*I and obphC-rev-*Pst*I with pLEBD4 [25] as a template. The resulting amplicon was cloned into pGYM [26] using *Nco*I and *Pst*I, generating pLEBD10. A *Sma*I site was introduced into the middle of the *bphC* gene of pLEBD10 using the oligo obphC-*Sma*I which creates a silent mutation in the codons specifying Pro_{130} and Gly_{131}. The *Sma*I/*Pst*I *bphC* gene fragment was then subcloned in pEMBL18 [27] to generate pFVBC54. Using pFVBC54 as a template, a total of six mutations were introduced in the *bphC* gene (see Table 1) using site-directed mutagenesis. The double variant V148L/A200I was generated using two rounds of mutagenesis and an additional subcloning step in pEMBL18 to regenerate the *Eco*RI site for elimination during the second mutagenesis reaction. Mutations were confirmed by DNA sequencing, then the *bphC* expression vector (derivatives of pLEBD4 [25]) were regenerated in a two-step procedure. First, full-length *bphC* mutants were generated by cloning the *Sma*I/*Pst*I fragment from derivatives of pFVBC54 (encoding the second half of DHBD) into pFVBC66. The latter is a derivate of pBluescriptII SK+ that lacks the vector's *Cla*I site and that contains the *Xba*I/*Sma*I *bphC* fragment (encoding the first half of DHBD) from pLEBD10 with the silent *Sma*I mutation. The resulting derivatives of pFVBC66 contained full-length, mutated *bphC* genes. Second, the 836 bp *Cla*I/*Hin*dIII fragment (a *Cla*I site is present at bp 129 of *bphC*) was cloned from each pFVBC66 derivative into a derivative of pLEBD4 in which the second half of *bphC* was removed. Each DHBD variant was produced in *P. putida* KT2442 [28] freshly transformed with the corresponding pLEBD4 derivatives essentially as previously described [14].

Purification and handling of DHBD samples. Buffers were prepared using water purified on a Barnstead NANOpure UV apparatus to a resistivity of greater than 17 MΩ cm. All manipulations involving the DHBD variants were performed under an inert atmosphere unless otherwise specified, usually in a Mbraun Labmaster glovebox (Stratham, NH) maintained at 2 ppm O_2 or less. The DHBD variants were purified and flash-frozen in liquid nitrogen for long-term storage as described previously [14]. Aliquots of DHBD variants were thawed immediately prior to use and were exchanged into 20 mM 4-(2-hydroxyethyl)-1-piper-

Table 1
Sequences of the oligonucleotides used in this study

Oligo name	Sequences (5′–3′)
obphC-for-*Nco*I	GGGCCATGGGCATCAGAAGTTTGG
obphC-rev-*Pst*I	CGGCTGCAGGGCTGTAGTAA
obphC-*Sma*I	GACACGGCCGCCCCGGGCAGGAACG
oODM	AGCTCGAATTGGTAATCATGG
obphC-V148L	ACGCAGCGCAGGAAATGCCCC
obphC-V148W	AACGCAGCGCCAGAAATGCCCC
obphC-M175W	CCCCATTTTCCAGTCGATGAC
obphC-A200I	AGCGGGAATGCGATAATTGCCAGGG
obphC-A200W	CGGGAATGCCCAAATTGCCAG
obphC-P280W	CCACATGCTCCAACTGTCGTGCC

Restriction sites are underlined and mutations introduced in the *bphC* gene are in bold.

azinepropanesulfonic acid (HEPPS), 80 mM NaCl ($I = 0.1$), pH 8.0, by gel filtration chromatography [14] unless otherwise stated. When necessary, samples of DHBD variants were further diluted using the same buffer. Protein concentrations were determined using the Bradford method [29]. Iron concentrations were determined colorimetrically using Ferene S [30].

Kinetic measurements and analysis of steady-state data. Enzymatic activity was routinely measured by following the consumption of dioxygen using a Clark-type polarographic O_2 electrode (Yellow Springs Instruments, Model 5301) as previously described [14,20]. All experiments were performed using 20 mM HEPPS, 80 mM NaCl ($I = 0.1$), pH 8.0, 25.0 ± 0.1 °C. Concentrations of active DHBD variants in the assay were defined by the iron content of the injected purified enzyme solution and were used in calculating specificity, catalytic and inactivation constants. The O_2 electrode was calibrated using standard concentrations of wild-type DHBD and DHB.

For specificity experiments in which the concentration of catecholic substrate was varied in air-saturated buffer, the initial velocities were analyzed using an equation describing a mechanism in which substrate inhibition occurs [14] or to the Michaelis–Menten equation [31], as appropriate. In each case, the substrate concentration and reaction velocities were monitored after the initiation of the reaction (10–20 s) and compared to calculated values to reject assays involving greater than 15% inactivation of the enzyme [14,20].

The steady-state cleavage of 3-Cl catechol by DHBD variants could not be directly followed using the oxygen electrodes due to the very slow rate of catalysis. The K_{mA}^{app} of DHBD variants for 3-Cl catechol was determined using DHB as a reporter substrate in the oxygen electrode assay as previously described [20]. The data were fit to an equation identical in form to that for competitive inhibition [31]. In this equation, the K_{mA}^{app} of 3-Cl catechol replaces the competitive inhibition constant, K_{ic}. All fitting was performed using the least squares and dynamic weighting options of LEONORA [31].

Stability in the presence of O_2 and mechanism-based inactivation studies. The stability of the free enzyme in the presence of O_2 was studied by incubating DHBD variants in the oxygraph cuvette under standard assay conditions, and monitoring A_t, the activity remaining after different time intervals, by adding DHB to the cuvette. The apparent first-order rate constant of inactivation, j_1^{app}, was determined as previously described using Eq. (1) [20], in which A_{max} is the activity observed in the absence of pre-incubation

$$A_t = A_{max} e^{-j_1^{app} t}. \quad (1)$$

Partition ratios for all substrates were determined using an oxygraph assay according to standard procedures [20]. The amount of DHBD added to the reaction cuvette was such that the enzyme was completely inactivated before 15% of either the catecholic substrate or O_2 was consumed in the reaction mixture. The partition ratio was calculated by dividing the amount of product formed by the amount of active DHBD added to the assay.

The apparent rate constant of inactivation during catalytic turnover in air-saturated buffer, j_3^{app}, was calculated from the partition ratio determined using the oxygraph assay under saturating substrate conditions ($[S] >> K_m$) according to established procedures (Eq. (2)) [20], except for 3-Cl catechol. Under such conditions, the concentration of free enzyme, [E], is negligible, and the partition ratio is equal to the ratio of the catalytic constant, k_{cat}^{app}, and the inactivation constant j_3^{app} (i.e., $\sum j_i = j_3$) [20]

$$\text{partition ratio} = \frac{\text{no. of substrate molecules consumed}}{\text{no. of enzyme molecules inactivated}} = \frac{k_{cat}}{\sum j_i}. \quad (2)$$

The rate constant of inactivation, j_3^{app}, for 3-Cl catechol was evaluated from j_S using Eq. (3) and DHB as a reporter substrate [20]. The latter was determined from progress curves obtained spectrophotometrically at 434 nm from reactions performed at saturating substrate concentrations, S, using Eq. (4) [20]

$$j_S = \frac{j_3^{app}[\text{3-CC}]}{K_{m3CC}^{app}(1 + [\text{DHB}]/K_{mDHB}^{app}) + [\text{3-CC}]}, \quad (3)$$

$$P_t = P_\infty(1 - e^{-j_S t}) + P_i. \quad (4)$$

In Eq. (3), K_{m3CC}^{app} and K_{mDHB}^{app} are the apparent K_m for 3-Cl catechol and DHB, respectively, in air-saturated buffer and j_S at each concentration of 3-Cl catechol and DHB was determined using Eq. (4). In Eq. (4), P_i and P_∞ are the concentrations of product at the start and end of the assay, respectively.

HPLC analyses. The partition ratio for 3-Cl catechol and the distal ring-cleaved product of 3-Cl catechol was determined by HPLC as described previously [20]. The solvent system previously described for the distal ring-cleaved product of 3-Cl catechol [20] was used to identify the distal ring-cleaved product of 3-Me catechol.

Results and discussion

Rationale for the choice of active site variants

We hypothesized that optimization of DHB cleavage by DHBD has resulted in an active site that is poorly complementary to catechol because the volume in the active site occupied by the second ring of biphenyl is excess "free" volume when catechol binds. The poor specificity of DHBD for catechol and the partial occupancy observed in the catechol:DHBD crystal structure support this hypothesis [14]. We therefore investigated the effect of modifying the size of the active site pocket on the reactivity of the enzyme with bicyclic and monocyclic catecholic substrates. Residues were targeted for substitution based on their location relative to the DHB rings in the enzyme-DHB crystal structure [14,15]. The substrate pocket is lined with hydrophobic residues. With the exception of catalytic residues, the proximal (catecholic) ring is lined with F187, N243, and P280. The distal ring is lined with V148, M175, A200, F202, and H209 (Fig. 2). The rings of DHB are relatively unencumbered as no residue is closer than 3.25 Å of

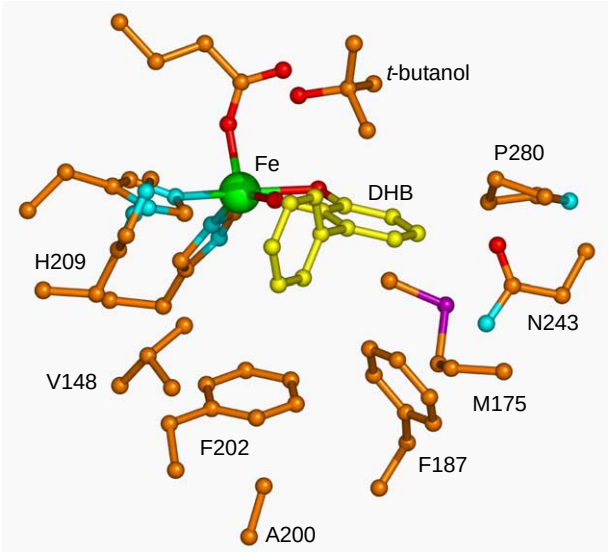

Fig. 2. View of the active site of DHBD bound to DHB. The DHB carbons are colored yellow. Other carbon, oxygen, nitrogen, sulfur, and iron atoms are colored orange, red, cyan, purple, and green, respectively. The ligands of the ferrous iron are H146, H210, and E260. For clarity, only one of the two possible orientations of M175 is shown. Adapted from [14,15]; figure made using Pymol [38].

C4, C5, and C6 of bound DHB. C3′, C4′, and C5′ of the distal ring are oriented towards the opening of the active site and therefore are even less sterically hindered. To get a good coverage of the active site, four residues were chosen to be modified: V148, M175, A200, and P280. Sequence alignments revealed that the positions corresponding to V148 and A200 are occupied by larger residues in several C23Os. For example, in C23O from *P. putida* mt-2 [16], a Leu is present at the equivalent position of V148 and an Ile at the equivalent position of A200. The following variants were generated: V148L, V148W, M175W, A200I, A200W, P280W, and V148L/A200I.

Purification and iron content

All variants were purified anaerobically using the procedure developed for the wild-type enzyme [14]. The proteins were estimated to be greater than 95% pure by SDS–polyacrylamide gel electrophoresis. The yield of each purified variant (10–20 mg/liter of cell culture) was typically lower than for the wild-type enzyme (30 mg/liter) [14]. All variants eluted as homooctamers on the Superdex 200 gel filtration column. No change in tertiary structure was observed but almost all variants showed a decrease in solubility. Typically, they tended to precipitate at concentrations higher than 7 mg/mL. By contrast, wild-type enzyme is soluble at concentrations above 40 mg/mL. The iron content of the wild-type enzyme typically ranges from 70 to 85% depending on the preparation. The iron content of the variants was always higher, ranging from 80 to 95% in all preparations. This high iron content strongly suggests that the iron ligands are in the correct configuration and thus that all variants were correctly folded. This conclusion was further substantiated for the V148L/A200I double variant, whose CD spectrum was essentially identical to that of WT-DHBD (data not shown). It is possible that a decrease in the size of the active site pocket stabilizes the active site iron, perhaps by minimizing exposure to solvent or inactivating agents.

Steady-state kinetic analysis

Steady-state kinetic analyses were performed in air-saturated buffer with each variant using catechol and DHB as substrates (Table 2). Because the K_m of DHBD for O_2 is approximately four times greater than the concentration of dissolved O_2 in the assay mixture [14], all kinetic parameters reported here are apparent. All variants were less specific for DHB than WT-DHBD, possessing apparent specificity parameters in the following order: WT-DHBD > A200I > V148L > V148L/A200I > M175W > A200W > V148W > P280W. The largest reduction of the k_{cat}^{app} value (12-fold) was observed with the V148W variant. Five of the variants were subjected to the same degree of substrate inhibition by DHB as the WT enzyme; substrate inhibition in the V148L/A200I double variant was fivefold stronger and was not observed at all in the M175W variant. The K_{mA}^{app} values were in a similar range for all variants, except for P280W that showed a 420-fold increase and could not be saturated with DHB.

In contrast to what was observed for DHB, four of the variants possessed a higher specificity for catechol than WT-DHBD. The apparent specificity constant for catechol was in the following order: V148W > V148L/A200I > A200I > V148L > A200W ~ WT-DHBD > M175W > P280W. However, all variants had lower k_{cat}^{app} values, from a threefold reduction for V148W to a 21-fold reduction for P280W. No substrate inhibition was observed for any of the variants and an increase in K_{mA}^{app} value was observed only for M175W and P280W when compared to WT-DHBD. The largest reductions in K_{mA}^{app} values were observed for the V148L/A200I (5-fold) and V148W (20-fold) variants.

The two variants that showed the biggest improvement in specificity for catechol, V148W and V148L/A200I, were further investigated using 3-Me catechol and 3-Cl catechol

Table 2
Apparent steady-state kinetic parameters of DHBD variants for DHB and catechol

Substrate	DHBD	K_{mA}^{app} (μM)	K_{iA}^{app} (mM)	k_{cat}^{app} (s^{-1})	k_{A}^{app} ($\times 10^6$ M^{-1} s^{-1})
DHB	WT[a]	12 (1)	3.0 (0.8)	251 (6)	21 (1)
DHB	V148L	13 (2)	1.1 (0.2)	190 (30)	14 (3)
DHB	A200I	13.1 (0.7)	2.0 (0.4)	220 (20)	17 (1)
DHB	V148L/A200I	13 (1)	0.6 (0.1)	77 (7)	6 (1)
DHB	V148W	17 (2)	2.2 (0.5)	21 (1)	1.2 (0.1)
DHB	M175W	21 (1)	—	97 (1)	4.6 (0.2)
DHB	A200W	19 (2)	1.0 (0.1)	66 (2)	3.6 (0.2)
DHB	P280W	5000 (1000)	1.5 (0.4)	280 (50)	0.055 (0.002)
Catechol	WT[a]	860 (150)	—	51 (6)	0.060 (0.004)
Catechol	V148L	350 (20)	—	32 (2)	0.091 (0.008)
Catechol	A200I	270 (40)	—	45 (3)	0.17 (0.02)
Catechol	V148L/A200I	165 (5)	—	38.9 (0.4)	0.236 (0.006)
Catechol	V148W	44 (5)	—	15.6 (0.3)	0.35 (0.04)
Catechol	M175W	1700 (100)	—	39 (1)	0.0227 (0.0008)
Catechol	A200W	360 (30)	—	21.8 (0.7)	0.060 (0.004)
Catechol	P280W	36000 (5000)	—	2.4 (0.3)	0.000070 (0.000003)

Experiments were performed using air-saturated 20 mM HEPPS, 80 mM NaCl, pH 8.0, at 25 °C. Values in parentheses represent standard errors.
[a] Data taken from [14].

Table 3
Apparent steady-state kinetic an inactivation parameters of DHBD and two variants for different substrates

DHBD	Substrate	K_{mA}^{app} (μM)	K_{iA}^{app} (mM)	k_{cat}^{app} (s^{-1})	k_A^{app} ($\times 10^6$ M^{-1} s^{-1})	Partition ratio	j_3^{app} ($\times 10^{-3}$ s^{-1})	j_3^{app}/K_{mA}^{app} ($\times 10^3$ M^{-1} s^{-1})
WT[a]	DHB	12 (1)	3.0 (0.8)	251 (6)	21 (1)	84,900 (1400)	3.0 (0.1)[b]	0.25 (0.10)
WT[a]	3-Me-catechol	530 (30)	—	97 (3)	0.2 (0.1)	5300 (300)	18 (2)[b]	0.035 (0.005)
WT[a]	Catechol	860 (150)	—	51 (6)	0.060 (0.004)	1230 (70)	42 (7)[b]	0.05 (0.02)
WT[b]	3-Cl-catechol	4.8 (0.7)	—	4 (1)	0.8 (0.4)	8 (2)	500 (20)	100 (20)
V148L/A200I[c]	DHB	13 (1)	0.6 (0.1)	77 (7)	6 (1)	1020 (60)	75 (10)	6 (1)
V148L/A200I	3-Me-catechol	200 (100)	0.3 (0.1)	300 (100)	1.3 (0.3)	1600 (100)	170 (90)	0.8 (0.9)
V148L/A200I[c]	Catechol	165 (5)	—	38.9 (0.4)	0.236 (0.006)	230 (30)	170 (20)	1.0 (0.2)
V148L/A200I	3-Cl-catechol	2.2 (0.5)	—	1.6 (0.7)[d]	0.7 (0.5)[d]	5 (2)[e]	330 (10)	150 (40)
V148W[c]	DHB	17 (2)	2.2 (0.5)	21 (1)	1.2 (0.1)	16,900 (300)	1.3 (0.1)	0.08 (0.02)
V148W	3-Me-catechol	15 (2)	2.6 (0.7)	21.1 (0.6)	1.37 (0.09)	7800 (100)	2.7 (0.1)	0.18 (0.02)
V148W[c]	Catechol	44 (5)	—	15.6 (0.3)	0.35 (0.04)	6400 (100)	2.4 (0.1)	0.055 (0.009)
V148W	3-Cl-catechol	1.6 (0.2)	—	1.3 (0.2)[d]	0.8 (0.2)[d]	9 (1)[e]	140 (5)	90 (20)

Experiments were performed using air-saturated 20 mM HEPPS, 80 mM NaCl, pH 8.0, at 25 °C. Values in parentheses represent standard errors.
[a] K_{mA}^{app}, K_{iA}^{app}, k_{cat}^{app}, k_A^{app}, and partition ratio data taken from [14].
[b] Data taken from [20].
[c] K_{mA}^{app}, K_{iA}^{app}, k_{cat}^{app}, and k_A^{app} data taken from Table 2.
[d] Values calculated by multiplying the partition ratio by j_3^{app} to obtain k_{cat}^{app} (Eq. (2)) and by dividing the calculated k_{cat}^{app} by K_{mA}^{app} to obtain k_A^{app}.
[e] Average of values obtained by oxygraph and HPLC assays.

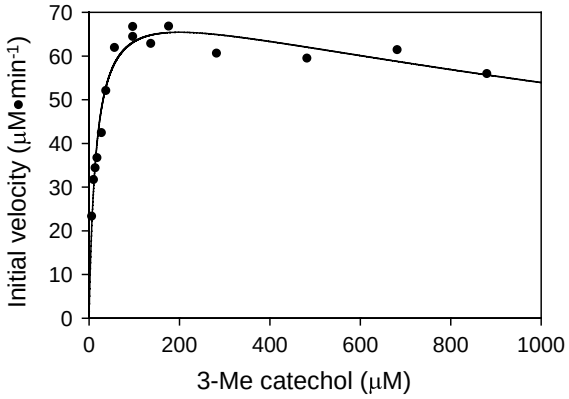

Fig. 3. Steady-state cleavage of 3-Me catechol by the V148W variant of DHBD. The line represents a best fit of the substrate inhibition equation to the data. The fitted parameters are $K_{mA}^{app} = 15 \pm 2$ μM, $K_{iA}^{app} = 2.6 \pm 0.7$ μM, and $V = 76 \pm 3$ μM/min. The experiment was performed using air-saturated 20 mM HEPPS, 80 mM NaCl, pH 8.0 ($I = 0.1$), 25 °C.

as substrates. In addition, the inactivation parameters for these variants in the presence of each of four tested substrates were evaluated (Table 3). With respect to WT-DHBD, both variants showed a ~7-fold increase in apparent specificity for 3-Me catechol and no change in specificity for 3-Cl catechol. The k_{cat}^{app} value of the V148L/A200I variant for 3-Me catechol was threefold higher whereas the same value of the V148W variant was fivefold lower. Both variants had lower K_{mA}^{app} values for 3-Me or 3-Cl catechol; the largest change was observed for the V148W variant, whose K_{mA}^{app} value for 3-Me catechol was 35-fold lower (Fig. 3). Finally, the substrate inhibition observed in the presence of 3-Me catechol was strong for the V148L/A200I variant but weak for the V148W variant.

As is typical of extradiol dioxygenases, DHBD is susceptible to inactivation during steady-state turnover in a process that involves dissociation of superoxide from the ternary complex [20]. Compared to WT-DHBD, V148L/A200I was more susceptible to inactivation (higher j_3^{app}/K_{mA}^{app}) with all substrates. In contrast, the V148W variant was only more susceptible to inactivation with 3-Me catechol and was actually less susceptible to inactivation with DHB. Moreover, the rate constant of inactivation (j_3^{app}) was decreased with all substrates for V148W whereas it was increased for all substrates except 3-Cl catechol for V148L/A200I, when compared to WT-DHBD.

Coupling of the reaction and stability in the presence of O_2

The coupling of DHB and catechol cleavage, respectively, with O_2-utilization in V148W and V148L/A200I was investigated using an O_2 electrode that had been calibrated using DHB and WT-DHBD, a well-coupled system [14]. For each variant, the amount of O_2 consumed corresponded to the amount of DHB and catechol added to the reaction mixture, demonstrating that the utilization of DHB and catechol was tightly coupled to O_2-consumption in both variants.

The stability of each variant in the presence of O_2 was evaluated by determining j_1^{app}, the pseudo-first-order rate constant of inactivation in air-saturated buffer. The respective j_1^{app} values of V148W and V148L/A200I were $(0.9 \pm 0.1) \times 10^{-3}$ s^{-1} and $(2.4 \pm 0.2) \times 10^{-3}$ s^{-1}, which correspond to half-lives of 13.1 ± 1.2 and 4.9 ± 0.5, respectively. In comparison, j_1^{app} of WT-DHBD is $(0.7 \pm 0.1) \times 10^{-3}$ s^{-1}; this corresponds to a half-life of 16 ± 2 min [20].

Distal ring-cleaved product of 3-Cl catechol

Some extradiol dioxygenases cleave certain catechols proximally (2,3-cleavage) and distally (1,6-cleavage) [32,33]. We therefore investigated the amount of distally cleaved product formed by the V148W and V148L/A200I variants, respectively, for each of 3-Cl and 3-Me catechol using HPLC and the previously described solvent system [20]. 3-Chloro-2-hydroxymuconic semialdehyde, the distal cleavage product of 3-chlorocatechol, constituted $1.8 \pm 0.3\%$ and $0.8 \pm 0.3\%$ of the ring-cleaved products in reactions catalyzed by the V148W and V148L/A200I variants, respectively. In comparison, the distal ring-cleaved product accounted for $1.8 \pm 0.1\%$ of the initial amount of 3-Cl catechol in the reaction catalyzed by WT-DHBD [20]. For 3-Me catechol, the distal ring-cleaved product constituted 0.5–0.6% of the reaction products regardless of which of the three enzymes was used as the catalyst. Therefore, the amino acid substitutions did not significantly affect the regiospecificity of the cleavage reaction. This result is in good agreement with a study on DHBD from *Sphingomonas xenophaga* BN6, an enzyme that preferentially catalyzes the distal cleavage of 3-Cl catechol [32]. When residues of this enzyme were replaced with smaller ones in a random mutagenesis study [33], an increase in distal product formation was observed. The regiospecificity of cleavage is likely determined by the orientation of the catecholic ring within the substrate-binding pocket. When the pocket allows for binding of the catechol in both orientations, it is likely that both distal and proximal cleavage can occur. Substitution of DHBD residues in the vicinity of C4 of the DHB ring with smaller residues might increase the yield of the distal cleavage product.

Structure-based interpretation of kinetic data

Crystal structures of DHBD from *B. xenovorans* LB400 have been reported for the substrate-free enzyme as well as for the binary complexes with each of catechol, 3-Me catechol, and DHB [13–15]. Crystal structures of other type I extradiol dioxygenases have been reported, including those of DHBD from *Pseudomonas* sp. KKS102 (substrate-free, a DHBD:DHB binary complex and a DHBD:DHB:NO ternary complex in which NO acts as an O_2 analog) [34,35], C23O from *P. putida* mt-2 (substrate-free) [16], and two homoprotocatechuate 2,3-dioxygenases (substrate-free and homoprotocatechuate-bound) [36]. DHBD from *Pseudomonas* sp. KKS102 is very similar to DHBD from *B. xenovorans* LB400 (66% sequence identity). Unsurprisingly, the structure and residues of the respective active sites of these two enzymes are especially similar. Of the four residues substituted in this study, two are identical (Val148 and Ala200) and two are conservatively replaced (M175 and P280 are Ile and Thr, respectively, in the KKS102 enzyme). Moreover, the residues contributing to the O_2-binding pocket, deduced from the DHB:DHBD:NO complex of the KKS102 enzyme [35], are identical, corresponding to residues H146, V148, F187, H195, A198, and H210 in the LB400 enzyme. In the KKS102 enzyme, the residue undergoing the largest movement upon NO binding is the valine, whose side-chain shifts by about 0.5 Å to accommodate the NO molecule. This observation correlates well with the results from the current study in which the V148W variant had significant reductions in k_{cat}^{app} for all substrates tested. This is likely due to a reduction in the size of the O_2-binding pocket caused by the replacement of V148 by a Trp. This change could interfere with the binding of O_2 to the iron to form the ternary complex as well as the orientation of the bound O_2 within the ternary complex. The relatively high K_m of DHBD for O_2 prevented direct testing of this hypothesis.

The specificity results are also consistent with the location of the residues in the substrate pocket. P280 interacts with the catecholic ring of DHB and its substitution for a larger residue dramatically reduces the specificity for both DHB and catechol. The P280W substitution must therefore cause a dramatic decrease in the pocket size for the catecholic ring and therefore interfere with its binding to iron and/or its reactivity with O_2 when bound to iron. In addition, P280 forms a hydrogen bond with H241. The introduction of a larger residue at position 280 could therefore influence the kinetic parameters by altering the positioning of H241, a residue that is thought to assist in the deprotonation of catechol as it binds to the iron [15].

The characteristics of the M175W variant are harder to rationalize. The M175 residue interacts with the distal ring of DHB but is located in close proximity of the catecholic ring. The M175W substitution also causes a decrease in specificity with DHB and catechol. Therefore, the position of the Trp residue must also interfere with binding of the catecholic ring and/or its reactivity with O_2 when bound to iron.

Residues V148 and A200 are located further away from the catecholic ring. Their substitution for larger residues showed a decrease in specificity for DHB and an increase in specificity for catechol in good agreement with the hypothesis that filling of the "free" volume occupied by the distal ring of DHB (when bound) increases specificity for smaller substrates. This hypothesis is also supported by the structure of C23O in which Leu and Ile residues are present at position equivalent to V148 and A200, respectively. Similarly, these residues are Ile and Gly, respectively, in a dioxygenase that preferentially cleaves 3-Me catechol and whose structure was recently modeled [37].

Structures of two homoprotocatechuate 2,3-dioxygenase:substrate complexes [36] reveal that the catecholic ring is accommodated by a binding pocket that is similar in shape to those of the DHBDs and C23O but that in the former, charged residues are also present to interact with the carboxylate of the homoprotocatechuate. In addition, the active site pocket possesses a well-defined lid domain that is much abbreviated in DHBD to accommodate the distal ring of DHB [36].

The influence of the substitutions of residues in the substrate-binding pocket of DHBD on the rate constant of inactivation (j_3^{app}) indicates that the latter is affected by the orientation of the bound catechol. This is most easily appreciated in the V148L/A200I variant as the lower j_3^{app} values of the V148W variant, with respect to those of WT-DHBD, likely reflect decreased reactivity with O_2 as discussed above for the k_{cat}^{app} values. The higher j_3^{app} values of the V148L/A200I variant are reminiscent of the higher j_3^{app} values of the WT-DHBD in the presence of sub-optimal substrates such as catechol and 3-Me catechol [20]. In both cases, higher j_3^{app} values may reflect reorientation or the lack of rigidity of bound substrate. Nevertheless, crystallographic data indicate that the orientation of hydroxylated rings of bound DHB, 3-Me catechol, and catechol in WT-DHBD:substrate complexes is very similar [14,15], indicating that the effect of structure on j_3^{app} is subtle.

Conclusion

This study demonstrates that the size of the active site pocket affects the type of catecholic substrate that can be cleaved by extradiol dioxygenases. Thus, the specificity of DHBD for catechol may be increased by replacing residues in the vicinity of the distal ring of DHB by larger ones. In the studied variants, the efficiency of cleavage was nevertheless reduced, likely because the introduced substitutions affected the O_2-binding pocket as well. The results further indicate that by influencing the orientation of the bound catecholic substrate, the binding pocket also helps minimize oxidative inactivation of the enzyme during catalysis.

Acknowledgments

Jeffrey T. Bolin is thanked for helpful discussion. This work was supported by grants from the Natural Sciences and Engineering Research Council of Canada (NSERC). F.H.V. was the recipient of Li Tze Fong Memorial and NSERC postgraduate scholarships.

References

[1] M. Boll, G. Fuchs, J. Heider, Anaerobic oxidation of aromatic compounds and hydrocarbons, Curr. Opin. Chem. Biol. 6 (2002) 604–611.
[2] B. Schink, B. Philipp, J. Muller, Anaerobic degradation of phenolic compounds, Naturwissenschaften 87 (2000) 12–23.
[3] F.H. Vaillancourt, J.T. Bolin, L.D. Eltis, Ring-cleavage dioxygenases, in: J.L. Ramos (Ed.), Pseudomonas, vol. III. Biosynthesis of Macromolecules and Molecular Metabolism, Kluwer Academic/Plenum Publishers, New York, 2004, pp. 359–395.
[4] S. Harayama, M. Rekik, Bacterial aromatic ring-cleavage enzymes are classified into two different gene families, J. Biol. Chem. 264 (1989) 15328–15333.
[5] O. Hayaishi, K. Hashimoto, Pyrocatechase: a new enzyme catalyzing oxidative breakdown of pyrocatechin, J. Biochem. 37 (1950) 371–374.
[6] Y. Kojima, N. Itada, O. Hayaishi, Metapyrocatechase: a new catechol-cleaving enzyme, J. Biol. Chem. 236 (1961) 2223–2228.
[7] L. Que Jr., M.F. Reynolds, Manganese(II)-dependent extradiol-cleaving catechol dioxygenases, Met. Ions Biol. Syst. 37 (2000) 505–525.
[8] L.D. Eltis, J.T. Bolin, Evolutionary relationships among extradiol dioxygenases, J. Bacteriol. 178 (1996) 5930–5937.
[9] K. Sugimoto, T. Senda, H. Aoshima, E. Masai, M. Fukuda, Y. Mitsui, Crystal structure of an aromatic ring opening dioxygenase LigAB, a protocatechuate 4,5-dioxygenase, under aerobic conditions, Struct. Fold. Des. 7 (1999) 953–965.
[10] R.N. Armstrong, Mechanistic diversity in a metalloenzyme superfamily, Biochemistry 39 (2000) 13625–13632.
[11] J.A. Gerlt, P.C. Babbitt, Divergent evolution of enzymatic function: mechanistically diverse superfamilies and functionally distinct suprafamilies, Annu. Rev. Biochem. 70 (2001) 209–246.
[12] M. Bergdoll, L.D. Eltis, A.D. Cameron, P. Dumas, J.T. Bolin, All in the family: structural and evolutionary relationships among three modular proteins with diverse functions and variable assembly, Protein Sci. 7 (1998) 1661–1670.
[13] S. Han, L.D. Eltis, K.N. Timmis, S.W. Muchmore, J.T. Bolin, Crystal structure of the biphenyl-cleaving extradiol dioxygenase from a PCB-degrading pseudomonad, Science 270 (1995) 976–980.
[14] F.H. Vaillancourt, S. Han, P.D. Fortin, J.T. Bolin, L.D. Eltis, Molecular basis for the stabilization and inhibition of 2,3-dihydroxybiphenyl 1,2-dioxygenase by *t*-butanol, J. Biol. Chem. 273 (1998) 34887–34895.
[15] F.H. Vaillancourt, C.J. Barbosa, T.G. Spiro, J.T. Bolin, M.W. Blades, R.F. Turner, L.D. Eltis, Definitive evidence for monoanionic binding of 2,3-dihydroxybiphenyl to 2,3-dihydroxybiphenyl 1,2-dioxygenase from UV resonance Raman spectroscopy, UV/Vis absorption spectroscopy, and crystallography, J. Am. Chem. Soc. 124 (2002) 2485–2496.
[16] A. Kita, S. Kita, I. Fujisawa, K. Inaka, T. Ishida, K. Horiike, M. Nozaki, K. Miki, An archetypical extradiol-cleaving catecholic dioxygenase: the crystal structure of catechol 2,3-dioxygenase (metapyrocatechase) from *Pseudomonas putida* mt-2, Struct. Fold. Des. 7 (1999) 25–34.
[17] P. Cerdan, A. Wasserfallen, M. Rekik, K.N. Timmis, S. Harayama, Substrate specificity of catechol 2,3-dioxygenase encoded by TOL plasmid pWW0 of *Pseudomonas putida* and its relationship to cell growth, J. Bacteriol. 176 (1994) 6074–6081.
[18] K. Furukawa, K. Tonomura, A. Kamibayashi, Effect of chlorine substitution on the biodegradability of polychlorinated biphenyls, Appl. Environ. Microbiol. 35 (1978) 223–227.
[19] S. Dai, F.H. Vaillancourt, H. Maaroufi, N.M. Drouin, D.B. Neau, V. Snieckus, J.T. Bolin, L.D. Eltis, Identification and analysis of a bottleneck in PCB biodegradation, Nat. Struct. Biol. 9 (2002) 934–939.
[20] F.H. Vaillancourt, G. Labbé, N.M. Drouin, P.D. Fortin, L.D. Eltis, The mechanism-based inactivation of 2,3-dihydroxybiphenyl 1,2-dioxygenase by catecholic substrates, J. Biol. Chem. 277 (2002) 2019–2027.
[21] T. Ishida, H. Tanaka, K. Horiike, Quantitative structure–activity relationship for the cleavage of C3/C4-substituted catechols by a prototypal extradiol catechol dioxygenase with broad substrate specificity, J. Biochem. (Tokyo) 135 (2004) 721–730.
[22] S. Nerdinger, R. Marchhart, P. Riebel, C. Kendall, M.R. Johnson, C.-F. Yin, V. Snieckus, L.D. Eltis, Directed ortho-metalation and Suzuki–Miyaura cross-coupling connections: regiospecific synthesis

of all isomeric chlorodihydroxybiphenyls for microbial degradation studies of PCBs, Chem. Commun. 1999 (1999) 2259–2260.
[23] F.M. Ausubel, R. Brent, R.E. Kingston, D.D. Moore, J.G. Seidman, J.A. Smith, K. Struhl, Current Protocols in Molecular Biology, J. Wiley & Sons Inc., New York, 2000.
[24] W.P. Deng, J.A. Nickoloff, Site-directed mutagenesis of virtually any plasmid by eliminating a unique site, Anal. Biochem. 200 (1992) 81–88.
[25] V. de Lorenzo, L.D. Eltis, B. Kessler, K.N. Timmis, Analysis of *Pseudomonas* gene products using *lacI*^{q}/*Ptrp-lac* plasmids and transposons that confer conditional phenotypes, Gene 123 (1993) 17–24.
[26] J.G. Guillemette, Y. Matsushima-Hibiya, T. Atkinson, M. Smith, Expression in *Escherichia coli* of a synthetic gene coding for horse heart myoglobin, Protein Eng. 4 (1991) 585–592.
[27] L. Dente, R. Cortese, pEMBL: a new family of single-stranded plasmids for sequencing DNA, Methods Enzymol. 155 (1987) 111–119.
[28] M. Herrero, V. de Lorenzo, K.N. Timmis, Transposon vectors containing non-antibiotic resistance selection markers for cloning and stable chromosomal insertion of foreign genes in gram-negative bacteria, J. Bacteriol. 172 (1990) 6557–6567.
[29] M.M. Bradford, A rapid and sensitive method for the quantitation of microgram quantities of protein utilizing the principle of protein-dye binding, Anal. Biochem. 72 (1976) 248–254.
[30] B.E. Haigler, D.T. Gibson, Purification and properties of NADH-ferredoxin$_{NAP}$ reductase, a component of naphthalene dioxygenase from *Pseudomonas* sp. strain NCIB 9816, J. Bacteriol. 172 (1990) 457–464.
[31] A. Cornish-Bowden, Analysis of Enzyme Kinetic Data, Oxford University Press, New York, 1995.
[32] U. Riegert, G. Heiss, P. Fischer, A. Stolz, Distal cleavage of 3-chlorocatechol by an extradiol dioxygenase to 3-chloro-2-hydroxymuconic semialdehyde, J. Bacteriol. 180 (1998) 2849–2853.
[33] U. Riegert, S. Burger, A. Stolz, Altering catalytic properties of 3-chlorocatechol-oxidizing extradiol dioxygenase from *Sphingomonas xenophaga* BN6 by random mutagenesis, J. Bacteriol. 183 (2001) 2322–2330.
[34] Y. Uragami, T. Senda, K. Sugimoto, N. Sato, V. Nagarajan, E. Masai, M. Fukuda, Y. Mitsui, Crystal structures of substrate free and complex forms of reactivated BphC, an extradiol type ring-cleavage dioxygenase, J. Inorg. Biochem. 83 (2001) 269–279.
[35] N. Sato, Y. Uragami, T. Nishizaki, Y. Takahashi, G. Sazaki, K. Sugimoto, T. Nonaka, E. Masai, M. Fukuda, T. Senda, Crystal structures of the reaction intermediate and its homologue of an extradiol-cleaving catecholic dioxygenase, J. Mol. Biol. 321 (2002) 621–636.
[36] M.W. Vetting, L.P. Wackett, L. Que Jr., J.D. Lipscomb, D.H. Ohlendorf, Crystallographic comparison of manganese- and iron-dependent homoprotocatechuate 2,3-dioxygenases, J. Bacteriol. 186 (2004) 1945–1958.
[37] D. Kim, J.C. Chae, J.Y. Jang, G.J. Zylstra, Y.M. Kim, B.S. Kang, E. Kim, Functional characterization and molecular modeling of methylcatechol 2,3-dioxygenase from o-xylene-degrading *Rhodococcus* sp. strain DK17, Biochem. Biophys. Res. Commun. 326 (2005) 880–886.
[38] W.L. DeLano, The PyMOL Molecular Graphics System, DeLano Scientific, San Carlos, CA, 2002.